HYPERELASTIC MODEL FOR FORMING SIMULATIONS OF A NON-CRIMP 3D ORTHOGONAL WEAVE E-GLASS COMPOSITE REINFORCEMENT

J. Pazmino[a], S. Mathieu[b], V. Carvelli[a]*, P. Boisse[b], S.V. Lomov[c]

[a] *Department of Architecture, Built Environment and Construction Engineering, Politecnico di Milano, Piazza Leonardo Da Vinci 32, 20133 Milan, Italy*
[b] *Laboratoire de Mécanique des Contacts et des Solides UMR CNRS 5514, INSA de Lyon Bâtiment Jacquard, Rue Jean Capelle, 69621 Villeurbanne, France*
[c] *Department of Metallurgy and Materials Engineering, KU Leuven, Kasteelpark Arenberg 44, B-3001 Leuven, Belgium*
** corresponding author: valter.carvelli@polimi.it*

Keywords: 3D composite reinforcement, Forming, Finite element modelling.

Abstract

The knowledge of the material behavior and production parameters during forming process of textile composite reinforcements are important to determine the conditions for a successful manufacturing of a composite preform without defects. To address this knowledge numerical tools capable to predict the behavior of textile composite reinforcements during complex 3D shaping are extremely important. In this work, the hyperelastic constitutive model proposed in [1] *is improved to investigate the formability of a single layer E-glass non-crimp 3D orthogonal woven reinforcement (commercialized under trademark 3WEAVE® by 3Tex Inc.). Comparisons between experiments and numerical simulations of tetrahedron and double-dome draping processes demonstrated the adequacy of the adopted model to predict the mechanical behaviour of the non-crimp 3D woven reinforcement during complex shape forming.*

1. Introduction

In the last decades, textile reinforcements for composite structures have attracted the interest from both academia and industry, particularly due to their superior shaping characteristics compared with laminates [2]. Textile reinforcements are especially efficient to adapt to double-curved moulds, due to their typical characteristic of high resistance to deformation in the fiber directions, which results in a material that deforms primarily by in-plane shear [3]. Composite components with complex shapes can be obtained by liquid moulding processes. The first stage of such processes consists in forming a dry textile reinforcement, generally by a punch and die process, before thermoset resin injection. The final properties of a composite part are largely established during the shaping of the structure. In fact, the forming determines the fiber orientations and density, which influence directly the permeability of the preform, and thus the mechanical response of the composite part [4].
The knowledge of the material behaviour and production parameters during forming process are important to determine the conditions for a successful manufacturing of a composite preform without defects (e.g. wrinkles).

Different models have been developed to study shaping process of two-dimensional composite reinforcements, (see e.g. [5] and [6]). While, only few studies have focused their attention on 3D woven fabrics (see e.g. [1] and [7]). Their behaviour, due to the presence of through-thickness yarns, is specific. Thus, a model capable to describe all the mechanisms involved during such deformation process must be adopted. In [1] authors proposed a continuous hyperelastic constitutive model to simulate forming of a 3D layer to layer angle interlock reinforcement.
In this work, the hyperelastic constitutive model detailed in [1] is improved to study the formability of a single layer E-glass non-crimp 3D orthogonal woven reinforcement (commercialized under trademark 3WEAVE® by 3Tex Inc.), on two complex shapes, i.e. tetrahedral and double-dome. The input data for the constitutive model are the measurements of the in-plane shear, tension, transverse compression and transverse shear deformation response of the 3D reinforcement ([8] and [9]).
The obtained results point out a good agreement with the experiments of such forming process described in [10], and, therefore, the capability of the proposed constitutive model to predict the mechanical behaviour of the non-crimp 3D woven reinforcement during complex shaping.

2. Features of the non-crimp 3D orthogonal woven reinforcement

The material is a single layer E-glass non-crimp 3D orthogonal woven reinforcement (commercialized under trademark 3WEAVE® by 3Tex Inc.). The fiber architecture of the preform has three warp and four weft layers, interlaced by through thickness (Z-directional) yarns (Figure 1 [11]). The fabric construction results in a ~49%/~49%/~2% ratio of the fiber amounts (by volume) in the warp, weft and Z fiber directions, respectively. The fiber material is PPG Hybon 2022 E-glass. Some characteristics of the non-crimp 3D orthogonal weave reinforcement are listed in Table 1.
The reader is referred to [8], [9] and [10] for a detailed description of the mechanical behaviour and experimental formability tests of the non-crimp 3D woven reinforcement into complex shapes.

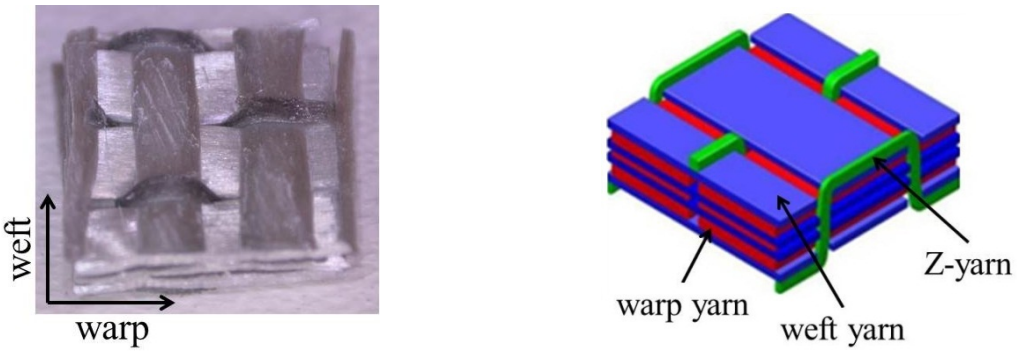

Figure 1. Architecture of the tows inside the non-crimp 3D orthogonal weave preform [11]: photo (left) and schematics (right) of the unit cell.

3. Continuous hyperelastic model

The continuous hyperelastic model, presented in [1] and used in this study, adopts as main deformation modes occurring during shaping and molding processes of 3D textile composite

reinforcements: (i) stretch in the warp direction; (ii) stretch in the weft direction; (iii) transverse compaction; (iv) in-plane shear; (v) transverse shear in the warp direction; and (vi) transverse shear in the weft direction. Transverse shear deformation is related to bending behavior of the reinforcement. In fact, bending is a deformation mode which involves transverse shear and, locally, longitudinal tension and compression.
The hyperelastic model assumes that the contribution of each deformation mechanism is independent from the others (i.e. neglects the probable coupling between different deformation modes). Therefore, for each deformation mode, a strain energy density function based on the experimental behavior of the reinforcement (i.e. experimental results presented in [8] and [9]), is defined. Afterwards, the strain energy density functions are used to determine the constitutive model parameters by fitting in the least-squares sense the calculated and experimental energies (i.e. strain energy potential) as described in [1].
The shape functions of the strain energy potentials allow a proper correlation between the experimental and the theoretical behavior [1]. Such functions have been improved in order to describe the mechanical behavior of the considered non-crimp 3D orthogonal weave E-glass composite reinforcement.

	Fabric plies	1
	Areal density (g/m^2)	3255
Warp	Insertion density (ends/cm)	2.76
	Top and bottom layer yarns (tex)	2275
	Middle layer yarns (tex)	1100
Weft	Insertion density (ends/cm)	2.64
	Yarns (tex)	1470
Z-yarns	Insertion density (ends/cm)	2.76
	Yarns (tex)	1800

Table 1. Properties of the non-crimp 3D orthogonal weave preform.

4. Some features of the finite element simulations

Forming process simulations of the non-crimp 3D orthogonal weave E-glass composite reinforcement into tetrahedral and double-dome shapes are detailed using Abaqus/Explicit finite element code [12]. This explicit analysis has been demonstrated to be suitable for non-linear geometric and material problems, in particular where a large number of contacts between the parts occur [3].
The tetrahedral and double-dome shape forming processes detailed in [10], are numerically simulated. The tools geometry, blank dimensions and test parameters used for finite element modelling are the same adopted in the experiments (see details in [10]). As shown in Figure 2, due to geometrical symmetry of the moulds, only half and quarter of the experimental set-up are considered for tetrahedron and double-dome numerical models, respectively. Blanks are discretized with hexahedral elements, while steel open dies and punches are treated as rigid bodies using four-node rigid elements. Finite element simulations are performed for two different mesh sizes (i.e. 3 and 5) to evaluate the effect of this parameter on the results.
Numerical analyses are carried out on blanks having the initial direction of the warp and weft parallel to the sides of the die (see Figure 2). Moreover, due to the importance of out-of-plane properties on the draping behavior of the 3D reinforcement (see [10]), the specimen thickness is discretized with four elements.

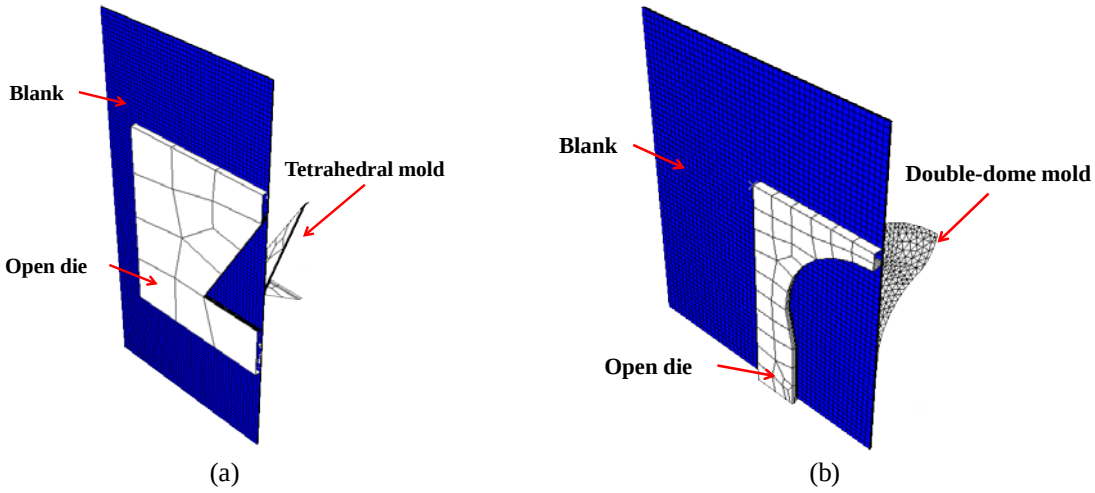

Figure 2. Finite element model for: (a) tetrahedron and (b) double-dome forming tests.

5. Finite element simulations results and comparison with experiments

The quasi-static response in the numerical analysis using an explicit numerical code is demonstrated with a negligible inertia effect. This requirement is satisfied when the kinetic energy (E_{kin}) of the blank is lower than 5% of the internal energy (E_{int}) , after a certain time of the deformation process ([3]).

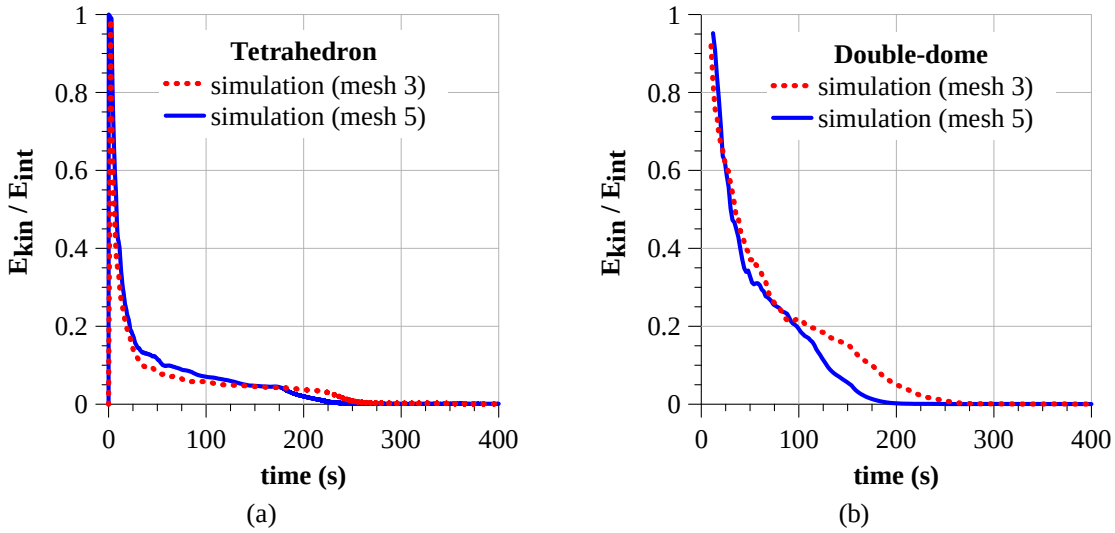

Figure 3. Ratio of kinetic (E_{kin}) to internal energy (E_{int}) of the blank during: (a) tetrahedron and (b) double-dome draping simulations.

Figure 3 depicts the ratio of kinetic (E_{kin}) to internal energy (E_{int}) of the blank, during tetrahedral and double-dome shape forming process simulations. The curves in Figure 3, for both element sizes adopted (i.e. 3 and 5), show that the kinetic to internal energy ratio of the blank is smaller than 5% after half of tetrahedron and double-dome shaping processes. This means that the finite element simulations are not affected by dynamic effects.

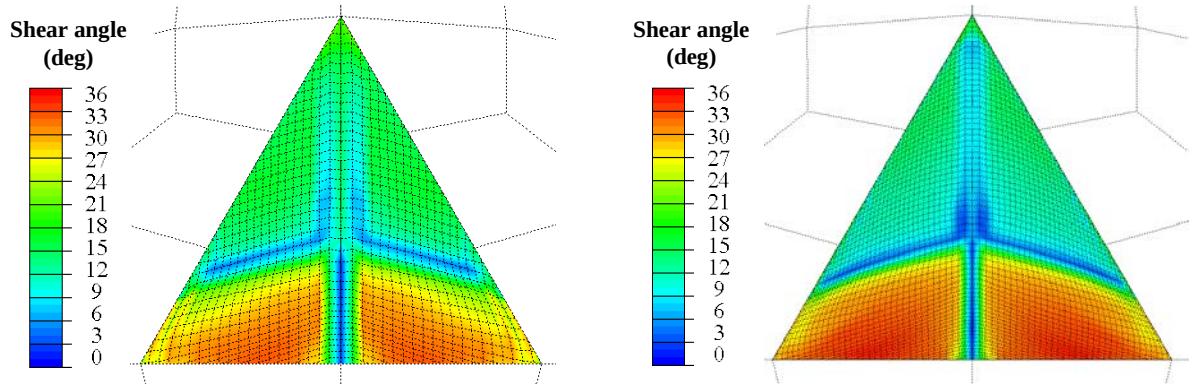

(a) (b)

Figure 4. Shear angle distribution at the end of tetrahedral mold shaping for numerical simulations with mesh size of: (a) 5 and (b) 3.

Being the shear one the main deformation mode during shaping, Figure 4 and Figure 5 illustrate the map of shear angle on the blank at the end of tetrahedron and double-dome draping processes, respectively. The plots demonstrate a negligible influence of the mesh size on the shear angle distribution.

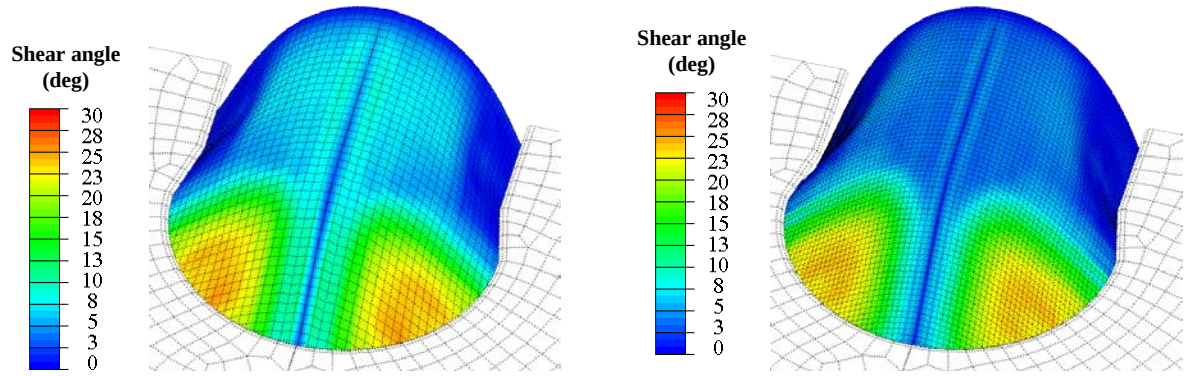

(a) (b)

Figure 5. Map of shear angles at conclusion of double-dome draping for numerical simulations with mesh size of: (a) 5 and (b) 3.

The experimental investigation detailed in [10] provides measurements of the shear angle distribution during the forming processes with the two moulds. The comparison of the finite element and experimental shear angle distribution are detailed in Figure 6a,b and Figure 7a,b at the end of tetrahedron and double-dome formability tests (i.e. mould displacement of ≈65 mm). The contour maps demonstrates agreement between experimental and numerical shear angles distribution on the entire external surface of the 3D fabric Moreover, shear angles are detailed along some selected paths (lines L1, L3 in Figure 6a and line L in Figure 7a). The numerical predictions in Figure 6c and Figure 7c show similar to the experimental maximum value of the local shear angle.

The absence of wrinkles observed in the experimental investigation (Figure 6d and Figure 7d) and in forming numerical simulations points out the capability of the adopted hyperelastic model to describe the correct deformation behavior of the non-crimp 3D orthogonal weave textile.

6. Conclusions

In this work, the hyperelastic model proposed in [1] is improved to study the formability of a single layer E-glass non-crimp 3D orthogonal woven reinforcement (commercialized under trademark 3WEAVE® by 3Tex Inc.) into tetrahedral and double-dome shapes. The input data for the material model are obtained by the experimental response of the 3D fabric under different deformation modes, presented in previous publications.
Finite element simulations and experimental results of tetrahedron and double-dome shaping processes demonstrated the adequacy of the adopted hyperelastic model to describe the deformation mechanisms involved during draping and the efficiency to predict the global behaviour of the non-crimp 3D woven reinforcement during complex shape forming.
The hyperelastic model, adopted in this study, provides an efficient numerical tool useful for the optimization of the forming process of any complex shape with such 3D reinforcement.

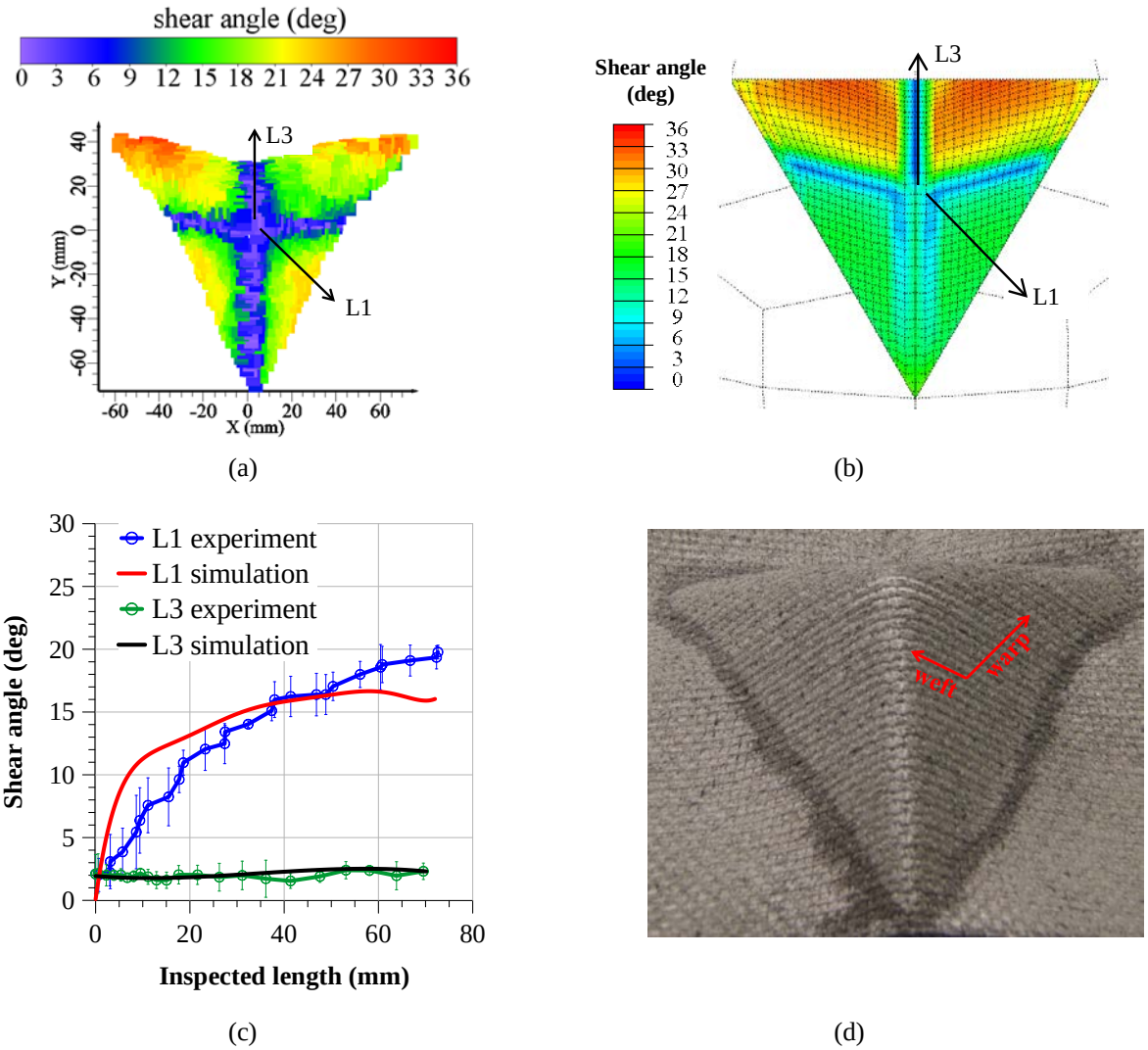

Figure 6. Tetrahedral shape forming test. Shear angle distribution at the end of draping process: (a) experimental (b) numerical simulation for a mesh size of 5; (c) along paths L1 and L3 (error bars give the standard deviation of four tests). (d) Experimental deformed shape of the 3D woven reinforcement.

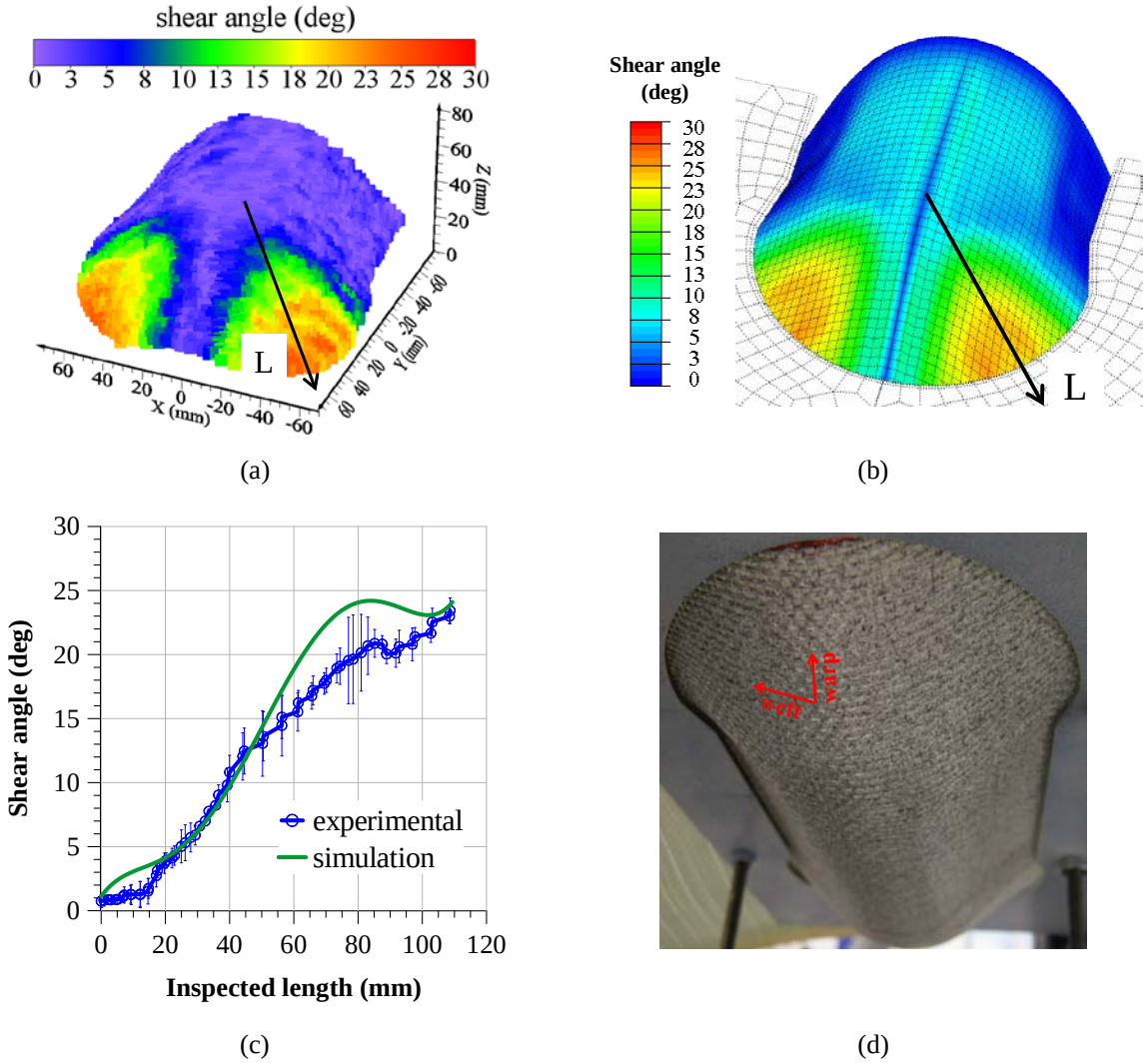

Figure 7. Double-dome forming tests. Shear angle distribution at the end of draping process: (a) experimental (b) numerical simulation for a mesh size of 5; (c) along line L (error bars give the standard deviation of four tests). (d) Experimental deformed shape of the 3D woven reinforcement.

References

[1] Charmetant A., Orliac J.G., Vidal-Sallé E. and Boisse P., "Hyperelastic model for large deformation analyses of 3D interlock composite preforms," *Composites Science and Technology*, vol. 72, p. 1352–1360, 2012.

[2] Long A.C., Design and manufacture of textile composites, New York. USA: Woodhead Publishing Limited & CRC Press LLC, 2005.

[3] Vanclooster K. , Lomov S.V. and Verpoest I., "Experimental validation of forming simulations of fabric reinforced polymers using an unsymmetrical mould configuration," *Composites: Part A* , vol. 40, pp. 530-539, 2009.

[4] Boisse P., Composite reinforcements for optimum performance, Woodhead Publishing Limited, 2011.

[5] Hamila N., Boisse P, Sabourin F. and Brunet M., "A semi-discrete shell finite element for textile composite reinforcement forming simulation," *International Journal for Numerical Methods in Engineering*, vol. 79, p. 1443–1466, 2009.

[6] Khan M.A., Mabrouki T., Vidal-Sallé E. and Boisse P., "Numerical and experimental analyses of woven composite reinforcement forming using a hypoelastic behaviour. Application to the double dome benchmark," *Journal of Materials Processing Technology,* vol. 210, pp. 378-388, 2010.

[7] De Luycker E., Morestin F., Boisse P. and Marsal D., "Simulation of 3D interlock composite preforming," *Composite Structures,* vol. 88, p. 615–623, 2009.

[8] Carvelli V., Pazmino J., Lomov S.V. and Verpoest I., "Deformability of a non-crimp 3D orthogonal weave E-glass composite reinforcement," *Composites Science and Technology,* vol. 73, pp. 9-18, 2012.

[9] Pazmino J, Carvelli V and Lomov S V, "Micro-CT analysis of the internal deformed geometry of a non-crimp 3D orthogonal weave E-glass composite reinforcement," *Composites Part B,* In printing. Published on line, 2013. DOI:10.1016/j.compositesb.2013.11.024..

[10] Pazmino J., Carvelli V. and Lomov S.V., "Formability of a non-crimp 3D orthogonal weave E-glass composite reinforcement.," *Composites Part A: Applied Science and Manufacturing.,* vol. 61, pp. 76-83, 2014.

[11] Carvelli V., Gramellini G., Lomov S.V., Bogdanovich A.E., Mungalov D.D. and Verpoest I., "Fatigue behaviour of non-crimp 3D orthogonal weave and multi-layer plain weave E-glass reinforced composites," *Composites Science and Technology,* vol. 70, pp. 2068-2076, 2010.

[12] Dassault Systemes - Abaqus/Explicit, http://www.3ds.com/products-services/simulia/portfolio/abaqus/abaqus-portfolio/abaqusexplicit/.